Estimates of CO emissions from open biomass burning in southern Africa for the year 2000

Akinori Ito[1] and Joyce E. Penner

Department of Atmospheric, Oceanic, and Space Sciences, University of Michigan, Ann Arbor, Michigan, USA

Received 13 August 2004; revised 8 August 2005; accepted 22 August 2005; published 14 October 2005.

[1] This paper compares the results of emission estimates of trace gases from open vegetation fires in southern hemisphere Africa for the year 2000 using different data sets. The study employs several approaches, deriving carbon monoxide (CO) emissions from a variety of satellite information, measurement data sets, and empirically-based techniques to estimate burned areas (BA), fuel consumption (FC), and emission factors (EF). Three BA data sets are used: the Moderate Resolution Imaging Spectroradiomter (MODIS) burned area data set, the Global Burned Area data set for the year 2000 (GBA2000), and the Global Burn Scar Atlas (GLOBSCAR) in July and September, 2000. The estimated total BA in southern Africa varies significantly among data sets from 210,000 to 830,000 km^2 for the sum of July and September. Temporal and spatial variations associated with CO emissions are analyzed using three different techniques for calculating the FC and EF. The first set of FC and EF extrapolates monthly variations in Zambia to southern Africa, the second extrapolates spatially resolved data for September to July, and the last includes monthly and spatial variations in both FC and EF. This analysis suggests the importance of accounting for the temporal and spatial variations in both FC and EF in order to determine the appropriate temporal and spatial variations of emissions from open vegetation fires. The CO emissions from open vegetation burning for the sum of July and September range from 18 to 31 Tg CO, using the MODIS BA data set and three different techniques for calculating FC and EF. The relative standard deviations (RSD) calculated from the three different methods are 58% for BA, 21% for FC, and 37% for EF. The best estimate of CO emissions from open biomass burning for the sum of the two months is 29 Tg CO, which may be compared to the estimates constrained by numerical models and measurements in 2000 which range from 22 to 39 Tg CO.

Citation: Ito, A., and J. E. Penner (2005), Estimates of CO emissions from open biomass burning in southern Africa for the year 2000, *J. Geophys. Res.*, *110*, D19306, doi:10.1029/2004JD005347.

1. Introduction

[2] Open biomass burning is one of the most significant sources of trace gases and aerosols on a global scale and contributes to high uncertainties in the estimates of pollutants in global chemistry transport models. The availability of satellite-based products to estimate spatial and temporal patterns of burned area provides an opportunity to use data sets depicting the spatial and temporal variations in fuel consumption and emission factors to determine biomass burning emissions. Using different satellite-based burned area data sets for the year 2000 [*Simon et al.*, 2004; *Tansey et al.*, 2004] and different methodologies, *Hoelzemann et al.* [2004] and *Ito and Penner* [2004] estimated global carbon monoxide (CO) emissions from open vegetation burning of 271 and 265 Tg CO year^{-1}, respectively. Although these two estimates are in good agreement on a global basis, they disagree on a regional scale and also disagree with inverse modeling studies (i.e., 552 Tg CO yr^{-1} from *Arellano et al.* [2004] and 408 Tg CO yr^{-1} from *Pétron et al.* [2004]) primarily because of variations in the estimates of area burned and fuel consumption [*Kasischke and Penner*, 2004]. Thus, a comparison between model estimates using satellite-based burned area data sets and measurements at a regional scale should be carried out in order to provide the user community with the means to assess the usefulness and uncertainty of the products from emission models. In this paper, we use a single general methodology [*Seiler and Crutzen*, 1980] but with several different data sets and models for emissions at a regional scale in order to both evaluate these data sets and models in conjunction with field measurements and to determine the most important issues to resolve.

[3] Detailed ground measurements of fuel and fire characteristics at a number of sites and airborne measurements

[1]Now at Frontier Research Center for Global Change, JAMSTEC, Yokohama, Japan.

0148-0227/05/2004JD005347

Table 1. Comparison of Annual Amounts of Areas Burned and CO Emissions From Open Vegetation Fires in Southern Africa Among Various Modeling Studies

Study	$[BA]$,[a] 10^6 km^2 yr^{-1}	$[FC] \times [EF]$,[b] kg CO m^{-2}	Emissions, Tg CO yr^{-1}
Scholes et al. [1996a, 1996b]	1.68	0.01	15
van der Werf et al. [2003]	1.16	0.13	147
Hoelzemann et al. [2004]	0.58	0.12	69
Ito and Penner [2004]	1.00	0.13	130
Palacios-Orueta et al. [2004]	1.08	0.20	218
Sinha et al. [2004]	0.77	0.03	26
Averages	1.04 ± 0.38	0.10 ± 0.07	101 ± 78
Relative standard deviations, %	36	68	78

[a]Burned area.
[b]Fuel consumption × emission factor (kg CO m^{-2}).

of trace species along several flight paths have been carried out in a variety of field campaigns, which have mainly focused on the Southern Hemisphere African savannas [*Lindesay et al.*, 1996; *Swap et al.*, 2003]. In order to calculate the overall production of gases from vegetation fires based on measurements, extrapolation of fire information from point measurements to the regional scale has conventionally been done by classifying the region into a number of vegetation types, estimating the mean fuel consumption and area burned, and then calculating the total amount burned [e.g., *Seiler and Crutzen*, 1980; *Hao et al.*, 1990]. However, an area the size of southern Africa has great heterogeneity with respect to fuel consumption. For example, field measurements of fuel consumption ranged from 0.15 to 0.60 kg dry matter (DM) m^{-2} during August and September 1992 at 13 sites in the South African and Zambian savannas [*Shea et al.*, 1996], and the fuel consumption varied seasonally from 0.14 to 0.31 kg DM m^{-2} at 7 sites in a dambo grassland and from 0.01 to 0.53 kg DM m^{-2} at 6 sites in a miombo woodland [*Hoffa et al.*, 1999]. Therefore, it may be difficult to represent the spatial and temporal distribution of the emissions using the conventional classification method which uses burned area data reported by local experts (or fire frequency) combined with the biomass available to burn and fraction of fuel load consumed during fires based on average data for different land covers and regions. For example, *Scholes et al.* [1996a] estimated 247–2719 Tg DM using a classification approach but only 90–264 Tg DM using a modeling approach. The modeling approach will be more accurate if it uses accurate space- and time-resolved burned area data coupled with realistic spatial and temporal variation in the biomass consumed. This is especially true for tropical regions in the Southern Hemisphere where reliable ground-based estimates of vegetation fire activity are rare. In any case, space-and-time-resolved data are needed to assess the environmental effect of trace gases and aerosols using atmospheric chemical transport models [e.g., *Kanakidou et al.*, 1999; *Penner et al.*, 2002].

[4] In general, the CO emissions per month ($[P]_{lm}$ g CO month^{-1}) at location l for month m from open vegetation fires can be described by the following equation [*Seiler and Crutzen*, 1980],

$$[P]_{lm} = [BA]_{lm} \times [FC]_{lm} \times [EF]_{lm} \quad (1)$$

where BA is the burned area per month m at location l (m^2 month^{-1}), FC is the fuel consumption (kg m^{-2}) expressed on a dry weight (DM) basis within each grid l, and EF is the emission factor in grams of CO per kilogram of dry matter burned. The annual amount of total area burned and CO emissions for southern Africa are compared among various modeling studies in Table 1. The estimates of area burned for southern Africa range from 0.58 to 1.68 (10^6 km^2 yr^{-1}), while those for emitted CO range from 15 to 218 Tg CO yr^{-1}. *Scholes et al.* [1996a] estimated ±49% errors in the biomass burned estimates, but none of the other estimates in Table 1 was within this range. Table 1 also shows the amount of CO emitted per unit area burned (kg CO m^{-2}) in order to examine differences based on the product of the fuel consumption and emission factors. The relative standard deviation (RSD) of CO emissions per unit area burned is 68% among these studies. While some of the variation in emissions among these studies may be due to interannual variability, some is undoubtedly due to different vegetation cover data sets and their assumed fuel loads. Since a variety of field measurements have become available for southern Africa [*Lindesay et al.*, 1996; *Swap et al.*, 2003], this region offers an excellent opportunity for evaluating modeling approaches at a regional scale. In addition, the outcome from the comparison between measurements and model results may suggest the necessity of field measurements in some parts of southern Africa to improve the emission estimates.

[5] The purpose of this paper is to determine open biomass burning emissions using different data sets and various approaches for estimating fuel consumption and emission factors and to evaluate the relative contributions of the factors that determine differences in these estimates of CO emissions. The uncertainties in spatially resolved data sets would have spatial variability [*Barrett et al.*, 2001], but this information is not available for the burned area data sets and fuel load maps. Therefore, it is not possible to carry out a formal error analysis at the present time. Instead, here we present an analysis of the sensitivity of the CO emissions to each factor in equation (1) to explore the relative importance of temporal and spatial variations in different treatments of BA, FC and EF for the determination of the overall emissions from open vegetation fires.

[6] Section 2 describes the data sets used for estimating the differences in the emissions associated with open vegetation burning. Section 3 compares different data sets for area burned, fuel consumption, and emission factors. The differences in temporal and spatial variations associated with FC and EF are analyzed based on models that predict the effects of fuel moisture and density on these factors with

Table 2. Summary of Data Sets and Parameterizations Used in the Estimation of Emissions From Open Vegetation Fires

Name[a]	Sources	Method and Satellite Information
BA1	*Roy et al.* [2002]	MODIS[b]
BA2	*Tansey et al.* [2004]	SPOT4[c]
BA3	*Simon et al.* [2004]	ATSR[d]
TCpre2	*Zhu and Waller* [2001]	Modified linear mixture model
TCpost3	*Hansen et al.* [2003]	Regression model
FVC	*Zeng et al.* [2000]	NDVI comparison
FC1	See Table 4	Compilation of measurements
FC2	*Hély et al.* [2003d]	Fuel consumption model
FC3	See Section 2.3	Fuel consumption model
EF1	See Table 4	Compilation of measurements
EF2	*Hély et al.* [2003d]	Regression model
EF3	See Section 2.4	Linear regression model

[a]TC, tree cover; FVC, fractional vegetation cover; FC, fuel consumption; EF, emission factor.
[b]MODIS, Moderate Resolution Imaging Spectroradiomter.
[c]SPOT, Systèm Pour l'Observation de la Terre.
[d]ATSR, Along Track Scanning Radiometer.

results that use monthly averaged measurements. Section 4 compares our different estimates of CO emissions from open vegetation burning with those estimated by numerical models and measurements from satellite data for the year 2000. Section 5 presents a summary of our findings including a description of the most uncertain factors in determining emissions from open biomass burning in southern Africa.

2. Data Sets Used to Estimate Open Biomass Burning Emissions

[7] In this study, the CO emissions per month ($[Q]_{hij}$ g CO month^{-1}) in a given grid box (m^{-2}) from open vegetation fires are described by the following equation,

$$[Q(\mathrm{CO})]_{hij} = [GA]_h \times [FC]_i \times [EF(\mathrm{CO})]_j \quad (2)$$

where *GA* represents the area burned (m^2 month^{-1}) in a given grid box for 3 different data sets (h = 3), *FC* is the fuel consumption per unit area of a grid box (kg m^{-2}) for three different data sets (i = 3). In addition, 3 different methods for determining the emission factors are applied (j = 3). Thus, these sets of data and methods provide 27 ($3 \times 3 \times 3$) estimates of emissions for each grid box. Our aim is to explore the sensitivity of the total emissions in Southern Africa to selected, reasonable, and different methodological assumptions in equation (2). We compare the FC and EF to measurements in order to recommend a best estimate and method for determining emissions.

[8] Table 2 summarizes the sources, methods, and satellite information for the data sets used in this work. Three burned area data sets from different satellite remote sensing products (BA1, BA2, and BA3) are available (see section 2.1). Two tree cover (TCpre and TCpost) and one fractional vegetation cover (FVC) data sets from different techniques are used to determine fuel load (see section 2.2). The fuel consumption is examined using three different data sets (FC1, FC2, and FC3) in each 1km grid of burned area (see section 2.3). For the purpose of the inter-comparison between measurements and models, one fuel consumption data set compiled from measurements (FC1) and the two fuel consumption models (FC2 and FC3) are examined. For FC3, to differentiate woodlands in which the trees are cut and burned from those in which this does not occur, a Tree Felled Factor (*TFF*) is developed using the difference between two different data sets of tree cover (TCpre and TCpost) (see section 2.3). Further, in FC3, the coarse fuel consumption in woodlands is determined from an assumed Residual Smoldering Factor (*RSF*), which represents whether or not the coarse fuels are consumed by residual smoldering fires [*Ito and Penner*, 2004]. To analyze seasonal and spatial variations in EF, three different estimates of emission factors (see section 2.4) are examined.

2.1. Area Burned Data Sets

[9] Burned area is defined as a fire scar detected by a satellite remote sensing instrument. These were provided at a resolution of either 0.5 km × 0.5 km or 1 km × 1 km with grid cells that were specified as either entirely burned or not burned at all. The fuels that actually burned (i.e., the fuel loads in vegetated areas and the fraction of actual consumption due to fires) are treated here as the fuel consumption in the grid cells associated with the resolution available from the burned area data set. *Simon et al.* [2004] and *Tansey et al.* [2004] summarized comparisons of two global area burned products, while *Korontzi et al.* [2004] compared three burned area products for southern Africa for September 2000. Here, we consider 3 burned area products for southern Africa in July and September. First, the Moderate Resolution Imaging Spectroradiometer (MODIS) burned area data set is available on the approximate day of burning at a 500 m resolution only for 2 months in July and September for the year of 2000 (designated BA1) on the third SAFARI 2000 CD-ROM [*Roy*, 2003]. In developing this data set, daily MODIS land surface reflectance data in the near-infrared (IR) and shortwave IR bands were used to discriminate between burned and unburned surfaces [*Roy et al.*, 2002]. We calculated the percentage of the total area burned of the 1 × 1 km grid from the 0.5 km grid of BA1 to estimate the CO emissions at 1 × 1 km grid [*Korontzi et al.*, 2004]. Second, the final version of the Global Burned Area data set for the year 2000 (GBA2000) was derived from ten-day composited reflection in the shortwave IR region from the VEGETATION instrument on board the Systèm Pour l'Observation de la Terre (SPOT) 4 satellite for the year

2000 (BA2) [*Tansey et al.*, 2004]. These global data were provided on a 1 km × 1 km grid resolution each month. Third, the Global Burn Scar Atlas (GLOBSCAR) data set is available on the approximate day of burning at a 1 km resolution (BA3) [*Simon et al.*, 2004]. This data set used the Along Track Scanning Radiometer (ATSR) data in the near IR, thermal IR, and shortwave IR to select burned surfaces.

2.2. Vegetation Cover Data Sets

[10] *Ito and Penner* [2004] compared three different tree cover data sets in order to estimate the fuels exposed to fires on a global scale. In this work, two of these data sets are used to develop an estimate of fuel exposed and burned in southern Africa. The first data set (TCpre) used AVHRR for 1995–1996 on a 1 km × 1 km grid resolution [*Zhu and Waller*, 2001], and the second data set (TCpost) used the MODIS satellite data set for 31 October 2000–9 December 2001 at a resolution of 0.5 km × 0.5 km [*Hansen et al.*, 2003]. TCpre (developed for the Forest Resources Assessment (FRA) 2000 report [*Saket*, 2001]) was produced using temporal compositing of AVHRR Normalized Difference Vegetation Index (NDVI) and a modified mixture analysis. TCpost was developed by employing continuous training data over the whole range of tree cover as opposed to a linear mixture model [*Hansen et al.*, 2002a]. The local validation in Zambia indicates an accuracy of ±5.2% [*Hansen et al.*, 2002b]. For our estimate of fuel consumed in July and September 2000 in FC3, TCpre is used as the tree cover before the fires and the TCpost is used as the tree cover after the fires.

[11] *Korontzi et al.* [2004] and *Sinha et al.* [2004] used two classifications of land cover types (i.e., woodlands and grasslands) to estimate the emissions from open vegetation fires in Southern Africa. In this study, land cover types are classified into two classes, based on the percentage of tree cover [*Di Gregorio and Jansen*, 2000; *Mayaux et al.*, 2004]. Woodlands were defined as those regions with greater than 15% tree cover, and grasslands were defined as those areas with less than or equal to 15% tree cover.

[12] A fractional vegetation cover data set is available on a global 1-km resolution and was derived from AVHRR NDVI data for 1992–1993, based on the annual maximum NDVI value for each pixel in comparison with the NDVI value that corresponds to 100% vegetation cover for each International Geosphere-Biosphere Programme (IGBP) land cover type [*Zeng et al.*, 2000]. The fractional herbaceous cover was derived from the difference between the fractional vegetation cover from *Zeng et al.* [2000] and the fractional tree cover but was constrained to be greater than zero [*Ito and Penner*, 2004]. Nevertheless, field studies should be used to improve these estimates.

2.3. Fuel Consumption

[13] Three primary maps of fuel consumption (FC) are constructed at a 1 km × 1 km resolution. The first is based on a scheme that uses available measurements and applies these to determine the average FC as in the classification method, while the second and third are based on different fuel consumption models.

[14] We first describe the conventional classification method and the measurements used for FC1. This scheme primarily relies on classifying the areas burned into either woodlands or grasslands. In July, the FC measured at 4 woodland sites in Zambia was 0.30 ± 0.16, while that at 3 grassland sites was 0.21 ± 0.07 kg DM m^{-2} [*Hoffa et al.*, 1999]. In September, the FC measured at 3 woodland sites in Zambia was 0.44 ± 0.01 kg DM m^{-2} [*Shea et al.*, 1996], while that at 9 grassland sites was 0.30 ± 0.08 kg DM m^{-2} [*Shea et al.*, 1996; *Hély et al.*, 2003a]. The woodland measurements quoted above for September include measurements in fallow Chitemene (0.44 kg DM m^{-2}), in moist Miombo woodland (0.42 kg DM m^{-2}) and in semiarid Miombo woodland (0.45 kg DM m^{-2}). Because the differences in fuel consumption measured at the three sites were insignificant in these different environments, we combined them into a single value to apply to our woodland vegetation cover category. These measurements include estimates of wood burning for all categories of fuels. Thus, they include coarse woody debris (CWD) as well as fine fuels. However, the measurements for July only include CWD with diameter up to 2.51 cm [*Hoffa et al.*, 1999]. For grasslands, *Hély et al.* [2003a] concluded that the two land cover types of dambo and flood plain did not differ in terms of fuel characteristics, fire behavior or combustion completeness. Thus, we used the averages of these two types for the fuel consumption in grasslands.

[15] The fire season in southern Africa typically starts in May in the northwest, moves southeast, and ends in October near the east coast of South Africa [*Cahoon et al.*, 1992]. Therefore, our estimates of fuel consumption are divided by latitude between the southern part of southern Africa (SSA <10°S) and the south equatorial part of Africa (SEA 0°–10°S). Figure 1 shows the seasonal variation of leaf area index (LAI) in the SSA and in the SEA. The dashed line represents the SEA, while the solid line denotes the SSA. These data are available at a spatial distribution of 16-km resolution on a monthly average basis [*Myneni et al.*, 1997]. The minimum of the LAI in the SEA was August, while that in the SSA was in September. This result indicates that the dry season in the SEA is earlier than that in the SSA. Therefore, we applied the FC measured during the end of the dry season in the SSA to July and September in the SEA. However, we note that the FC in the SEA in FC1 may be underestimated because the LAI in the SEA is larger than that in the SSA.

[16] The second fuel consumption data set (FC2) was based on the fuel loads and combustion factors generated by *Hély et al.* [2003b], and was applied to herbaceous vegetation and the fine litter associated with dead leaves and twigs, but does not include CWD. The modeled fuel loads (FL) for different vegetation types are available on the third SAFARI 2000 CD-ROM at a 1km resolution [*Hély et al.*, 2003c]. We note that since this data set does not include Madagascar, it is left out of our study as well. The fuel loads for herbaceous vegetation and dead leaves were derived from a one-year simulation of a net primary production (NPP) model, while those for small twigs were estimated from empirical relationships between small twigs and the tree cover percentage. The tree cover percentage used for this relationship was derived from an AVHRR data set for 1992–1993 [*Hansen et al.*, 2000]. We note that the total grass fuel load estimated by *Hély et al.* [2003b] is similar to those from field measurements from the Southern African Fire-Atmosphere Research Initiative (SAFARI-92) project

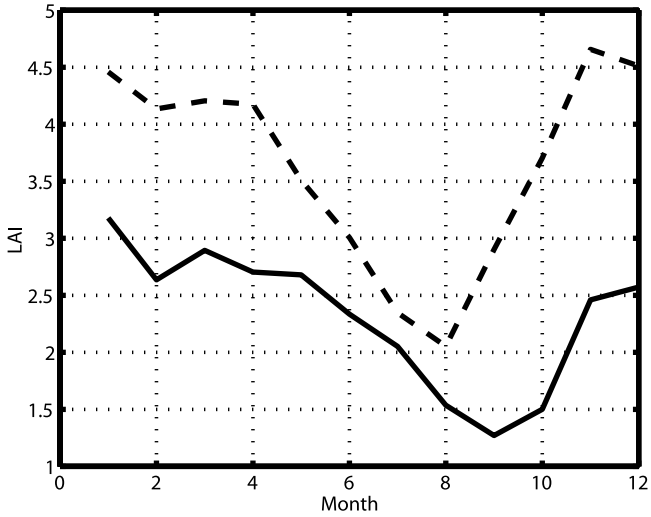

Figure 1. Seasonal variation of leaf area index in the southern part of southern Africa (SSA <10°S) and south equatorial Africa (SEA 0°–10°S). The dashed line represents the SEA, while the solid line denotes the SSA.

[*Shea et al.*, 1996] and from the Southern African Regional Science Initiative (SAFARI 2000) field campaigns [*Hély et al.*, 2003a] for tree cover estimates of 0, 30, and 50% [*Hély et al.*, 2003b]. An empirical relationship between the combustion factor (CF) and TC (correlation coefficient (r^2) = 0.54) was developed by *Hély et al.* [2003b] based on 32 data points during the dry season in a savanna ecosystem in southern Africa. The FC is calculated by multiplying the FL and CF.

[17] The third data set for fuel consumption (FC3) is formed from a combination and modification of FC2 and the FC model from *Ito and Penner* [2004]. Our fuel consumption model considers six elements: herbaceous vegetation, the fine litter pool of leaves and twigs, coarse woody debris, and above-stump leaves and wood. FC3 uses the biomass densities of the herbaceous vegetation, living leaves, living wood, and coarse woody debris from *Ito and Penner* [2004], small twigs from *Hély et al.* [2003b], and adds a modified version of the dead leaf fuel load from *Hély et al.* [2003b].

[18] In order to differentiate whether or not coarse fuels are burned in FC3, three different types of fire activities are defined for woodlands. *Hansen et al.* [2003] have shown that recent burn scars can be detected from a change in the tree cover percentage as determined from satellite image interpretation. Thus, we assumed that the fractional tree cover that burns in any given time period may be approximated from the difference between tree cover data sets from different years. (This assumes, of course, that both these tree cover data sets are accurate.) The trees in these areas were assumed to have been felled and the tree felled factor (*TFF)* at a given location, s, was estimated from the difference in tree cover before the fire, TCpre, and after the fire, TCpost.

$$[TFF]_s = \left([\mathrm{TCpre}]_s - [\mathrm{TCpost}]_s\right)/[\mathrm{TCpre}]_s \qquad \left(15\% < [\mathrm{TCpre}]_s\right) \tag{3}$$

The regions with larger than 15% tree cover that experienced a change in tree cover are assumed to have partially burned both the CWD as well as the felled (previously live) trees if the area is associated with a non-zero ATSR fire count [*Arino and Plummer*, 2001] and if the fuel is in a dry condition (which was prescribed by a temporally-varying CF). As in *Ito and Penner* [2004], we assumed that the ATSR fire counts detect long-lasting, smoldering fires, which consumed part of the CWD and the felled trees. If the tree cover did not change, two other fire activity assumptions for woodlands are made. If the area is associated with a non-zero ATSR fire count [*Arino and Plummer*, 2001], we assumed that it was subject to long-lasting, smoldering fires. These understory fires consume part of the CWD in the tree covered areas, but do not consume the living trees. If the area is not associated with a non-zero ATSR fire count, then we assume that the coarse fuels did not burn. Since the ATSR fire counts may not capture all smoldering fires (in part because of their low temperature at night) [*Simon et al.*, 2004], the contribution of the emissions from long-lasting fires to the total emission is expected to be underestimated. Here, we adopt these classifications for the fuel burn model used in FC3, and use field measurements (as evaluated in FC1) to evaluate the fuel consumption in FC3 in both woodlands and grasslands. We also examine the emission factors used in both these categories relative to measurements.

[19] The fuel consumption in FC3 is the product of the fuel load (FL) (kg DM m^{-2}) and the combustion factor (CF). In the following, we describe the data that we used to develop the FL and CF for FC3 which largely follows the study published by *Ito and Penner* [2004] but has been modified to include some of the elements from FC2.

[20] The biomass density for herbaceous vegetation in FC3 was based upon the relationship between the annual rainfall and in-situ biomass density measurements at about 150 sites in West African savannas from *Menaut et al.* [1991]. The r^2 for biomass as a function of rainfall was 0.7 [*Menaut et al.*, 1991]. The average biomass density (0.29 kg DM m^{-2}) in grasslands from 42 grassland sites distributed around the world was in good agreement with the estimate (0.24 kg DM m^{-2}) from the local long-term averages of annual precipitation at the same sites compiled by *Gill et al.* [2002] [*Ito and Penner*, 2004]. Thus, we applied this relationship to the data from July, 1999 to August, 2000 at a 2.5-degree resolution using monthly rainfall data from *Roads et al.* [2003] in southern Africa. The rainfall data were developed from the "best available" observations and models [*Roads et al.*, 2003]. The annual rainfall data were calculated from the 12 monthly data prior to the fires. The fuel load ($[FLf]_{it}$ kg DM m^{-2}) for each month, t, in each 1 km × 1 km cell, i, can be calculated from the herbaceous cover ($[Hc]_i$), which is related to the tree fraction, and the annual rainfall (AR mm) accumulated before each month, t,

$$[FLf]_{it} = [Hc]_i \times \left(4.9 \times 10^{-4} \times [AR]_{it} - 0.058\right). \tag{4}$$

As in *Ito and Penner* [2004], the herbaceous cover was estimated from TCpre and the fractional vegetation cover estimated by *Zeng et al.* [2000].

[21] As noted above, if the TFF is larger than zero, the fine fuels associated with felled trees are subject to partial

consumption. We estimated the living leaf biomass density from the above-ground tree biomass density at a 5-km resolution [*Brown and Gaston*, 1995] and the fraction of tree biomass density associated with leaves (9.3% for evergreen, 2.5% for deciduous forests, and 5.9% for mixed forests) [*Jenkins et al.*, 2001]. Forest areas for these three different vegetation types (evergreen, deciduous, and mixed forests) were derived from the 1 km grid IGBP land cover map [*Loveland et al.*, 2000]. In addition, the fire history was taken into account by using the ATSR hot spot record from 1996 to 2000 at a 1-km resolution [*Arino and Plummer*, 2001] and setting the fuel loads of the leaves attached to the felled trees to zero in each grid after a fire.

[22] The fine litter pool of dead leaves was estimated from the one-year net primary production model of *Hély et al.* [2003c] together with the estimated turn over time and fire history, rather than directly using the one-year estimate as in FC2. Thus, the fine fuel load production rate from the one-year net primary production model was converted to a litter pool by multiplying by the turn over time. The steady-state turn over time for the litter pool was estimated from measurements of the pool at 267 sites and the annual litter production rate at 754 sites from around the world by vegetation type [*Matthews*, 1997], and extrapolated using a vegetation map at a 1-degree resolution [*Matthews*, 1983]. *Matthews* [1997] outlined that the uncertainties and biases associated with her estimate of litter production and pools particularly arise from the following: (1) uncertainties inherent in the measurements, (2) identification of measured components such as leaf and wood, (3) natural spatial and temporal variability of production and pools, and (4) identification of the ecosystem represented by the measurements. The range for the turn over time was limited to 1 to 5 years [*Matthews*, 1997]. In addition, the fire history was taken into account by using the ATSR hot spot record from 1996 to 2000 at a 1-km resolution [*Arino and Plummer*, 2001] and resetting the litter pool to zero in each grid after a fire and adding the annual production each year until the steady state litter pool was reached. We note that ATSR fire counts could significantly underestimate savanna fires and that they tend to detect the longer lasting fires that are burning at night [e.g., *Boschetti et al.*, 2004]. However, the turn over time for the litter pool was not applied to savannas, because there was no available data for this type of vegetation in *Matthews* [1997]. Because the miombo understory burns about every two years [*Shea et al.*, 1996; *Desanker et al.*, 1997], and most dambos burn annually [*Hoffa et al.*, 1999], the lack of information on the accumulation of fuel loads for dead leaves in these savannas will not cause a significant error in our overall estimates. Nevertheless, measurements of the fire history at a fine resolution are needed to improve the estimates of the fuel loads for dead leaves accumulated over several years between two fire occurrences.

[23] Coarse fuels in the fuel load model associated with FC3 include the living woody biomass and coarse woody debris. As noted above, these are partially burned when the tree cover is reduced ($TFF > 0$) and fires are detected at night (ATSR fire count > 0) in dry conditions (temporally-varying CF for fine fuels > 47%). Following *Ito and Penner* [2004], the biomass density of coarse fuels was derived from the living above-ground wood biomass density [*Brown and Gaston*, 1995; *Jenkins et al.*, 2001] and from the ratio of coarse woody debris to the live wood biomass [*Harmon and Hua*, 1991; *Matthews*, 1997]. The ratios of CWD to live wood biomass reported by *Harmon and Hua* [1991] (5% for tropical rain forests, shrublands, and grasslands and ~20–25% for subtropical, temperate, and boreal forests) are extrapolated spatially using a vegetation map at a 1-degree resolution [*Matthews*, 1983]. In addition, the fire history was taken into account by using the ATSR hot spot record from 1996 to 2000 at a 1-km resolution [*Arino and Plummer*, 2001] to reduce the biomass density. Thus, we multiplied the FL by the CF after each fire occurrence in each grid and each year. We used the CF measured in fallow chitemene for this purpose (0.26 ± 0.06) [*Shea et al.*, 1996].

[24] For the fine fuels in grasslands and woodlands, we adopted a combustion factor that depends on the fuel moisture. Thus, we relate the combustion factor to the percentage of green grass out of the total grass (PGREEN) [*Hoffa et al.*, 1999]. The relationship for each CF was calculated based on the measurements at 8 sites presented by *Shea et al.* [1996], *Ward et al.* [1996], *Hoffa et al.* [1999], and *Korontzi et al.* [2003]. These measurements took place in Zambia from June to September.

[25] For dambo grasslands, we find

$$[\mathrm{CF}]_{it} = -1.976 \times [\mathrm{PGREEN}]_{it} + 1.3762 \qquad (r^2 = 0.709) \quad (5)$$

For miombo woodlands, we find

$$[\mathrm{CF}]_{it} = -2.1319 \times [\mathrm{PGREEN}]_{it} + 0.8736 \qquad (r^2 = 0.578) \quad (6)$$

[26] The range for the CF was limited to 0.44 to 0.99 for grasslands, while it was limited to 0.01 to 0.88 for woodlands. The monthly averaged PGREEN was calculated from the results of the NPP model of *Hély et al.* [2003d].

[27] As noted above, in some woodland regions (where $TFF > 0$), fires may consume a fraction of the coarse fuel load associated with trees. An average combustion factor of 0.26 ± 0.06 for coarse fuels with diameter >2.54 cm was calculated from measurements in fallow chitemene, where trees were cut and burned for the conversion of the land to pastures [*Shea et al.*, 1996]. Typically, the original trees are slashed and then burned by property owners at these sites towards the end of the dry season [*Desanker et al.*, 1997]. This value of CF was used for the coarse fuels in regions where $TFF > 0$. However, even though a fire scar is detected in a grid, it may not always mean that the felled trees and CWD in that grid are burned, especially if the fuel is in a wet condition. Field measurements showed that the coarse fuels were not burned when the CF for fine fuels was less than 47% in miombo woodlands [*Hoffa et al.*, 1999]. Therefore, we assume that the CF for coarse fuels is only activated when the temporally-varying CF for fine fuels is larger than 47%. In areas where smoldering fires occur (i.e. where the ATSR fire counts were detected), we defined a similar CF for the coarse woody debris. This was based on the average CF measured in the semiarid miombo woodland

(0.22 ± 0.22) [*Shea et al.*, 1996], and was similarly only activated when the CF for fine fuels was larger than 47%.

2.4. Emission Factors

[28] The amount of biomass burned together with the mode of burning (flaming or smoldering) is used to estimate emissions of carbon monoxide (CO). We use three different methods for determining the emission factors. The 3 methods are applied to each of our three fuel consumption models.

[29] The first method was based on the classification technique. This method uses monthly averaged emission factors from a compilation of measurements in different land cover types (designated EF1). In July for the SSA, the EF measured at 4 woodland sites in Zambia (78 ± 21 g-CO kg-DM^{-1}) was used in our woodlands category, while that measured at 3 grassland sites (43 ± 11 g-CO kg-DM^{-1}) [*Korontzi et al.*, 2003] was used in our grassland category. In September for the SSA and for both July and September for the SEA, the EF measured at 4 woodlands sites in September (76 ± 28 g-CO kg-DM^{-1}) was used in our woodlands category, while that measured at 2 grasslands sites (44 g-CO kg-DM^{-1}) [*Ward et al.*, 1996; *Yokelson et al.*, 2003] was used in our grasslands category. These average emission factors were extrapolated over the entire 1km grid in grasslands and woodlands in our FC1 model. To evaluate the EF models, we used the measurements of modified combustion efficiency (MCE) for the SSA in September from the same fires in woodlands (0.93 ± 0.02) and for those in grasslands (0.96) as those for the measured emission factors [*Ward et al.*, 1996; *Yokelson et al.*, 2003].

[30] The second EF data set (EF2) was generated using the fuel load data from *Hély et al.* [2003c] and the equations presented in *Hély et al.* [2003d]. *Hély et al.* [2003d] derived an empirical relationship between the ratio of the grass fuel load to the sum of litter and grass fuels present before the fire and MCE ($r^2 = 0.7954$), based on 13 data sets for the dry season [*Ward et al.*, 1992, 1996]. They also calculated a relationship between the MCE and EF.

[31] The third method for emission factors takes into account the type of combustion (e.g., flaming and smoldering fires). For this method, we used an approach based on relating the MCE to the EF of the fires (designated EF3) [*Ward et al.*, 1996]. Following *Hoffa et al.* [1999] we related the MCE to PGREEN in grasslands,

$$[\mathrm{MCE}]_{it} = -0.2116 \times [\mathrm{PGREEN}]_{it} + 1.0098 \qquad (r^2 = 0.6967) \tag{7}$$

while in woodlands, we developed a relationship between MCE and CF,

$$[\mathrm{MCE}]_{it} = -0.0422 \times [\mathrm{CF}]_{it} + 0.9458 \qquad (r^2 = 0.6232) \tag{8}$$

These two formulas were developed based on measurements at 8 sites taken from *Shea et al.* [1996], *Ward et al.* [1996], *Hoffa et al.* [1999], and *Korontzi et al.* [2003]. The relationships above include measurements obtained in both the early and late burning season.

[32] Measurements of MCE and EF taken from a wide variety of independent fire measurements varying from tropical to boreal zone fuels [*Hurst et al.*, 1994a, 1994b; *Andreae et al.*, 1996; *Ward et al.*, 1996; *Goode et al.*, 2000; *Shirai et al.*, 2003; *Yokelson et al.*, 2003] were used to develop a regression model between EF and MCE:

$$[EF(\mathrm{CO})]_{it} = -1134 \times [\mathrm{MCE}]_{it} + 135 \tag{9}$$

Because these measurements were mostly sampled by an aircraft, they may not sample the smoke from smoldering CWD and coarse fuels from felled trees. For this fuel, we used the EF measured for CWD [*Bertschi et al.*, 2003].

3. Results

3.1. Differences in Area Burned Products

[33] *Korontzi et al.* [2004] analyzed the spatial coincidences among BA1, BA2, and BA3, and discussed the importance of accurate burned area information not just in terms of the total area but also in terms of its spatial distribution. The sum of the total area burned from the BA1 data set (831 × 10^3 km^2) is substantially larger than that from either the BA2 (475 × 10^3 km^2) or the BA3 (210 × 10^3 km^2) data sets. Additionally, 337 × 10^3 km^2 of the burned area in BA1 is collocated with the area burned in BA2 and 126 × 10^3 km^2 is collocated with the area burned in BA3 at the 1-km grid. These results suggest that BA1 not only detects a larger number of areas burned, but also classifies 29% of the burned area in BA2 and 40% of the burned area in BA3 as not being burned. The ratios between the burned area in July and September indicate that BA3 shows the highest contribution of early dry season burning (July/September ratio of 2.5). BA2 and BA1 have ratios of 1.7 and 1.3, respectively.

3.2. Differences in Fuel Consumption

[34] We examined the implications of the FC model as a function of time and space. The FC1 model represents a spatial extrapolation of field measurements taken in Zambia, while the FC2 model is a temporal extrapolation of methods that were primarily based on field experiments at the end of the dry season. Here, we compare the FC from our three models to analyze the effect of temporal variations and the spatial distribution in FC. In the following comparisons for the analysis of temporal and spatial variations in FC, the BA1 data set is used for the burned area.

[35] The average fuel consumption estimates from the two models (FC2 and FC3) in July and September are compared to monthly averaged field measurements (FC1) in Table 3. The average estimates from FC1, FC2, and FC3 in woodlands (0.36–0.44 kg DM m^{-2}) are in good agreement (RSD = 11%) for the SSA in September, while that for FC3 (0.47 kg DM m^{-2}) in the SSA in July is larger than that from FC1 (0.30 ± 0.16 kg DM m^{-2}). However, field measurements of FC ranged from 0.16 to 0.53 kg DM m^{-2} in July, 1996 [*Hoffa et al.*, 1999], and FC3 is within this range. Although the average estimates from FC2 and FC3 in grasslands (0.44–0.48 kg DM m^{-2}) for the SSA are larger than that from FC1 (0.21–0.30 kg DM m^{-2}), the FC2 and FC3 in grasslands are within the natural variability in Zambia for the year 2000 (0.36–0.48 kg DM m^{-2}) [*Pereira et al.*, 2002]. In the SEA, the differences in woodlands are largest in July between FC1 (0.44 kg DM m^{-2}) and FC3

Table 3. Comparison of Fuel Consumption[a]

	July			September		
	Woodlands	Grasslands	All Lands	Woodlands	Grasslands	All Lands
SEA[b]						
FC1[c]	0.44	0.30	0.38	0.44	0.30	0.38
FC2	0.29	0.40	0.34	0.33	0.40	0.36
FC3	0.61	0.58	0.60	0.54	0.47	0.51
SSA[d]						
FC1[c]	0.30 ± 0.16	0.21 ± 0.07	0.26	0.44 ± 0.01	0.30 ± 0.08	0.36
FC2	0.33	0.44	0.38	0.36	0.44	0.40
FC3	0.47	0.48	0.47	0.44	0.44	0.44

[a]Units are in kg DM m^{-2}.
[b]South equatorial part of Africa (SEA 0°–10°S).
[c]Measured values pertain to regions of SSA but were extrapolated to SEA.
[d]Southern part of southern Africa (SSA <10°S).

(0.61 kg DM m^{-2}). Because the FC1 model in the SEA is extrapolated from the measurements at 3 Zambian woodlands sites in September, and because the LAI of the SEA is considerably larger than that for the SSA (see Figure 1), the spatial variations of fuel consumption associated with FC1 may be too small. The ecology of miombo ecosystems is closely related to that of the cerrado in South America [*Desanker et al.*, 1997]. The measurement of fuel consumption in cerrado (0.62 kg DM m^{-2}) [*Ward et al.*, 1992] is in good agreement with the FC3 model for woodlands in the SEA in July (i.e. 0.61 kg DM m^{-2}).

[36] This discussion shows the need to treat the fuel consumption as a function of time and space. Because the FC1 model is based on field measurements in the SSA, in applying them to the SEA, we are assuming that regional fuels in the burning season are the same. Because the FC2 model is based on field measurements at the end of the dry season, in applying them throughout the season, we are assuming that regional fuels in the burning season are sufficiently dry to ignore the dependence of FC on the fuel moisture content. However, ignoring the seasonal variation of FC between July and September in the SSA does not cause a significant error in the total emissions of CO because the differences between the FC measurements in July and September are within a standard deviation of the measurements in either month in woodland fires (Table 3) and woodland fires are a much larger source of CO than are grassland fires in southern Africa [*Korontzi et al.*, 2004; *Sinha et al.*, 2004]. Moreover, the fuel loads in the FC2 model were calculated for the year 2000 [*Hély et al.*, 2003b]. Nevertheless, the FC3 model is the only model that accounts for both seasonal and spatial variations in FC. In addition, this method accounts for the burning of CWD and the fuel associated with felled trees. To examine the impact of this additional fuel, we estimated the average FC for the FC3 model when the CWD and coarse fuels from felled trees were not included. The values with the coarse fuels are nearly the same as those from FC3 without the coarse fuels. *Shea et al.* [1996] reported that the majority of CWD had been previously removed for use as fuels prior to the fires by local farmers. This method (FC3) has employed strong constraints for burning the coarse fuels (i.e. ATSR fire count > 0) in order to capture this factor. However, some large diameter, downed logs may be subject to smoldering fires, especially further from villages where such logs are harder to utilize as fuel [*Yokelson et al.*, 2003]. This points out the need to measure the fuel consumption of coarse fuels for smoldering fires in southern Africa and determine the tree cover and change in tree cover from year to year. We also estimated the average FC for the leaves from felled trees. The average estimates for the leaves from FC3 for July (0.17 kg DM m^{-2}) and September (0.10 kg DM m^{-2}) in the SSA woodlands are in good agreement with the differences between FC2 and FC3 (0.14 and 0.08 kg DM m^{-2}, respectively). This comparison shows that most of the additional fuel consumption in FC3 for woodlands when these fuels are burned is associated with the burning of the leaves from felled trees. The 3-dimentional information associated with the location (i.e. latitude and longitude) and time of the burning of the leaves from felled trees as well as other fuels is not included in the average measurements of FC represented by FC1. This can account for some of the lack of ecosystem variation as well as the higher average FC in the FC3 model. Because the FC3 model is in reasonable agreement with the measured FC, and because it is able to account for both spatial and temporal variations, we conclude that the FC3 model is the best method to determine the FC among the three methods presented here.

3.3. Differences in Emission Factor

[37] Table 4 summarizes the emission factors from the three EF models used here. The average EF for CO from the EF3 model in the SSA for September (67 g-CO kg-DM^{-1}) compares well with that from the EF1 model (65 g-CO kg-DM^{-1}), while that from the EF2 model (101 g-CO kg-DM^{-1}) is larger than both of them. The average EF from the EF2 model in woodlands for the SSA in September (102 g-CO kg-DM^{-1}) is identical to that from the EF3 model, and is within the variability of the measurements used to determine the FC1 model (76 ± 28 g-CO kg-DM^{-1}). However, the average EF for the SSA in September from the EF2 model in grasslands (82 g-CO kg-DM^{-1}) is larger than that from the EF1 model (44 g-CO kg-DM^{-1}) and the EF3 model (35 g-CO kg-DM^{-1}). The average EF for the SSA in July from the EF3 model (35 g-CO kg-DM^{-1}) is within the variability of the measurements used for the EF1 model (43 ± 11 g-CO kg-DM^{-1}), while that from the EF2 model (88 g-CO kg-DM^{-1}) is larger than the upper end of the range from the measurements. The MCE for the EF2 model in woodlands for the SSA in September (0.90) is in good agreement with that for the EF1 model (0.93 ± 0.02) and the EF3 model (0.91), while that for

Table 4. Comparison of Emission Factors[a]

	July			September		
	Woodlands	Grasslands	All Lands	Woodlands	Grasslands	All Lands
SEA[b]						
EF1[c]	76	44	65	76	44	65
EF2	129	113	121	135	119	127
EF3	101	36	74	102	35	75
SSA[d]						
EF1[c]	78 ± 21	43 ± 11	64	76 ± 28	44	65
EF2	101	88	94	102	82	101
EF3	99	35	68	102	35	67

[a]Units are in g-CO kg-DM^{-1}.
[b]South equatorial part of Africa (SEA 0°–10°S).
[c]Measured values pertain to regions of SSA but were extrapolated to SEA.
[d]Southern part of southern Africa (SSA <10°S).

the EF2 model in grasslands (0.92) is smaller than that for the EF1 (0.96) and EF3 (0.97) models. The measured emission factors (i.e. EF1) are similar in July and September in both woodlands and grasslands, a feature that is captured well by both the EF2 and EF3 models. Because the EF3 model accounts for temporal and spatial variations in EF, and because it provides a good agreement with the measured values in the SSA, we conclude that the EF3 model is the best method for determining EF among the methods presented here.

4. Differences in CO Emissions

[38] In order to examine differences in bottom-up estimates of CO emissions from different data sets with those from top-down estimates, we compared the estimates of CO from the different combinations of the factors in equation (2) to the ranges deduced from the inverse modeling studies by *Arellano et al.* [2004] and *Pétron et al.* [2004] for the sum of July and September in 2000. In the former study, the annual amount of the prescribed CO emissions was optimized, so that the predicted annual average CO mixing ratios from a chemical transport model fit the measured CO mixing ratios for the year 2000 derived from the Measurements of Pollution in the Troposphere (MOPITT) instrument [*Arellano et al.*, 2004]. They specified monthly-varying CO emissions from biomass burning in 2000 using the data set from *van der Werf et al.* [2003], which incorporates satellite observations of fires, biogeochemical modeling of available biomass, and biome-specific CO emission factors. In the *Pétron et al.* [2004] study, the monthly amounts of the prescribed CO emissions were optimized, so that the predicted CO mixing ratios from a chemical transport model fit the measured monthly average CO mixing ratios for the year 2000 derived from the MOPITT instrument [*Pétron et al.*, 2004]. Biofuel emissions were separated from the open vegetation fire category in these studies [*Arellano et al.*, 2004; *Pétron et al.*, 2004] and thus are also not included here. Although the CO emissions from *Arellano et al.* [2004] were only constrained on an annual basis, the ratio of the sum of July and September to the annual emissions from the global estimate of *Ito and Penner* [2004] (0.44) are in good agreement with the a priori estimate of *van der Werf et al.* [2003] (0.45) and with the a posteriori estimate of *Pétron et al.* [2004] (0.43). Therefore we used the ratio of the a priori estimate for July and September to the total a priori measurement to determine the sum of the July and September CO emissions in southern Africa from the *Arellano et al.* [2004] annual estimates.

[39] In order to investigate the sensitivity of the CO emissions to each factor in equation (2), 4 sets of simulations are examined: (1) standard run, (2) sensitivity to BA, (3) sensitivity to FC, and (4) sensitivity to EF. Our estimates for CO emissions using the 3 BA, the 3 FC, and the 3 EF models are compared to those from the inverse studies in

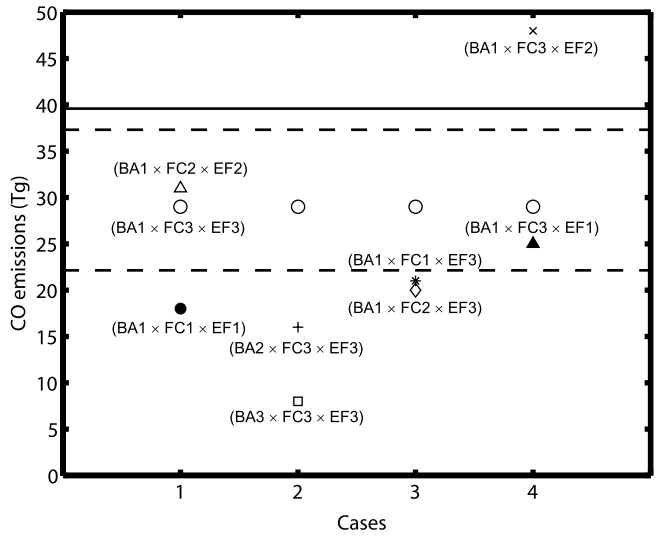

Figure 2. CO emissions (Tg CO) from open vegetation burning for sum of July and September in 2000. Case 1 examines the three main models studied here. The black circle represents (BA1 × FC1 × EF1), the white triangle represents (BA1 × FC2 × EF2), and the white circle represents (BA1 × FC3 × EF3). Case 2 examines the effect of variations in BA: the plus represents (BA2 × FC3 × EF3), while the square represents (BA3 × FC3 × EF3). Case 3 examines the effect of variations in FC. The asterisk represents (BA1 × FC1 × EF3), while the diamond represents (BA1 × FC2 × EF3). Case 4 examines variations in EF. The black triangle represents (BA1 × FC3 × EF1), while the cross represents (BA1 × FC3 × EF2). The horizontal line denotes the CO emission from monthly estimates [*Pétron et al.*, 2004], while the dashed lines denote the range of CO source strengths from annual estimates [*Arellano et al.*, 2004].

Figure 2. The black circle represents (BA1 × FC1 × EF1), the white triangle (BA2 × FC2 × EF2), the white circle (BA1 × FC3 × EF3), the plus (BA2 × FC3 × EF3), the square (BA3 × FC3 × EF3), the asterisk (BA1 × FC1 × EF3), the diamond (BA1 × FC2 × EF3), black triangle (BA1 × FC3 × EF1), and the cross (BA1 × FC3 × EF2). The horizontal line denotes the CO emissions from the monthly estimates of *Pétron et al.* [2004] (39 Tg CO), while the dashed lines denote the range of CO source strengths in July and September from the annual estimates of *Arellano et al.* [2004] (22–37 Tg CO). Because the NPP model results for fuel loads were not available for Madagascar and the emission in Madagascar is much smaller than that in southern Africa, we did not include bottom-up estimates of the CO emissions from Madagascar.

[40] First, let us examine the 3 models represented as case 1 in Figure 2. The estimates from two of the models (BA2 × FC2 × EF2: 31 Tg CO) and (BA1 × FC3 × EF3: 29 Tg CO) yield larger emissions than that from the method based on measurements of the FC and EF applied to different land use categories (BA1 × FC1 × EF1: 18 Tg CO). Nevertheless, the estimates of CO emissions from these two modeling approaches are in the middle of the range calculated by numerical models and measurements from the MOPITT instrument in 2000 (which are from 22 to 39 Tg CO) [*Arellano et al.*, 2004; *Pétron et al.*, 2004], while that based on simply extrapolating the measured FC and EFs is too low. While the true uncertainties from the inverse models are likely larger than the ranges shown in Figure 2, the comparisons of results from both atmospheric chemical transport models with surface CO measurements also support these source strengths [*Arellano et al.*, 2004; *Pétron et al.*, 2004].

[41] Second, let us examine the CO emissions when we vary the BA estimates (case 2 in Figure 2). The CO emissions from BA1 (BA1 × FC3 × EF3: 29 Tg CO) are compared with those from BA2 (BA2 × FC3 × EF3: 16 Tg CO) and from BA3 (BA3 × FC3 × EF3: 8 Tg CO). This sensitivity test results in the largest RSD of 58%.

[42] Third, let us examine the CO emissions when we vary the FC model. The CO emissions from FC3 (BA1 × FC3 × EF3: 29 Tg CO) are compared with those from FC1 (BA1 × FC1 × EF3: 21 Tg CO) and from FC2 (BA1 × FC2 × EF3: 20 Tg CO). The result from FC3 is larger than those from FC1 and FC2 by 8 and 9 Tg CO, respectively. The major additional component included in the FC3 model compared to that in the FC2 model is the leaf attached with the tree felled and burned (8 Tg CO). As noted above, this result suggests that the FC3 model is sensitive to the accuracy of tree cover data sets. This sensitivity test results in an RSD of 21%.

[43] Finally, the CO emissions from varying the EF model are compared in case 4. The CO emissions from EF3 (BA1 × FC3 × EF3: 29 Tg) are compared with those from EF1 (BA1 × FC3 × EF1: 25 Tg CO) and from EF2 (BA1 × FC3 × EF2: 48 Tg CO). The result from the EF1 model is in good agreement with that from EF3. This sensitivity test results in an RSD of 37%.

[44] We may further compare the combination of (BA1 × FC3 × EF3) with the monthly emissions for July and September and the geographical distribution in the SEA and the SSA from *Pétron et al.* [2004]. Our CO emissions in the SEA decreased from 12 Tg CO month^{-1} in July to 1 in September in the SEA, while those in the SSA increased from 7 Tg CO month^{-1} in July to 9 in September. These trends in the source strengths in the SEA and in the SSA are consistent with those deduced by *Pétron et al.* [2004] whose estimates vary from 13 to 10 and from 1 to 15, respectively, but the intensities are substantially different in the late burning season in the SEA and in the early burning season in the SSA. The tendencies of larger emissions in July than in September are in line with results from other burned area data sets (see section 3.1). *Pétron et al.* [2004] noted that there is a 1 to 2-month delay between the peak in the MODIS fire counts and the peak in the MOPITT CO retrievals for most regions in the southern hemisphere. Further studies are needed to investigate the differences between the peak of the burned area data and the CO retrieved from satellites.

5. Discussion and Conclusions

[45] Different burned area products, fuel consumption data, and emission factor models were examined for southern Africa. To estimate the emissions from open vegetation fires in Southern Africa in FC3, land cover types are classified into four classes based on the percentage of tree cover, the difference between tree cover data sets from different years, and the ATSR fire counts. In addition to the ranges in the total biomass subject to burning, the spatial and temporal variations associated with emissions of trace gases were analyzed using different techniques for calculating the combustion factors and emission factors. A spatially and temporally varying emission modeling approach is preferable to one that uses a non-varying space and/or time CF and EF.

[46] The most significant differences in the emissions associated with different data sets can be ascribed to differences in estimated burned area data sets in southern Africa (RSD 58%). The fuel consumption and emission factor models presented in this study were compared with a limited number of measurements. The FC3 and EF3 models were selected as the best models because they represent spatial and temporal variations and because their predicted FC and EF were within the ranges estimated by measurements. In addition, the FC3 model includes the burning of felled trees, which could be an important factor in total emissions. The average estimate from our best model, FC3, in woodlands is identical to that from measurements of FC1 (0.44 kg DM m^{-2}) for the southern part of southern Africa (SSA <10°S) in September, while the differences in woodlands are largest between FC1 (0.44 kg DM m^{-2}) and FC3 (0.61 kg DM m^{-2}) for the south equatorial part of Africa (SEA 0°–10°S) in July. In this context, field measurements of FC are required in the south equatorial part of Africa (SEA 0°–10°S) to improve the emission estimates in southern Africa.

[47] The ranges of total CO emissions associated with different combinations of factors were also compared to the ranges from inverse modeling studies for the year 2000. The estimated ranges from both the (BA2 × FC2 × EF2: 31 Tg CO) and (BA1 × FC3 × EF3: 29 Tg CO) modeling approaches for CO emissions from open biomass burning using the MODIS burned area data set [*Roy et al.*, 2002]

were within the range of the estimates constrained by chemical transport models and measurements for the year 2000 (22 to 39 Tg CO). Clearly, differentiation of different modeling methods for CO emission requires a high accuracy in the data sets for burned area. Moreover, the fuel consumption must be accurately determined. Since the total fuel consumed is determined by the combustion fraction times the fuel load, both these factors must be known accurately. We have also shown that the FC3 model is sensitive to the accuracy of tree cover data. Thus, the tree cover needs further validation and should be made available on monthly and annual basis if biomass burning estimates are to improve.

[48] **Acknowledgments.** We are grateful to the NASA Global Aerosol Climatology Program and the NASA Radiation Sciences Program as well as the DOE chemistry program. We thank the European Space Agency - ESA/ESRIN via Galileo Galilei, CP 64, 00044 Frascati, Italy, for providing the ATSR data and the Joint Research Centre (JSC), Ispra (VA), I-21020, Italy, for providing the GBA2000 data. The authors wish to thank the Oak Ridge National Laboratory Distributed Active Archive Center at Goddard Space Flight Center, USA, for producing the SAFARI 2000 data in its present format and distributing them.

References

Andreae, M. O., E. Atlas, H. Cachier, W. R. Cofer III, G. W. Harris, G. Helas, R. Koppmann, J.-P. Lacaux, and D. E. Ward (1996), Trace gas and aerosol emissions from savanna fires, in *Biomass Burning and Global Change*, edited by J. S. Levine, pp. 278–295, MIT Press, Cambridge, Mass.

Arellano, A. F., Jr., P. S. Kasibhatla, L. Giglio, G. R. van der Werf, and J. T. Randerson (2004), Top-down estimates of global CO sources using MOPITT measurements, *Geophys. Res. Lett.*, *31*, L01104, doi:10.1029/2003GL018609.

Arino, O., and S. Plummer (2001), Along Track Scanning Radiometer world fire atlas: Validation of the 1997–98 active fire product, Eur. Space Res. Inst., Eur. Space Agency, Frascati, Italy.

Barrett, D. J., I. E. Galbally, and R. D. Graetz (2001), Quantifying uncertainty in estimates of C emissions from above-ground biomass due to historic land-use change to cropping in Australia, *Global Change Biol.*, *7*, 883–902.

Bertschi, I., R. J. Yokelson, D. E. Ward, R. E. Babbitt, R. A. Susott, J. G. Goode, and W. M. Hao (2003), Trace gas and particle emissions from fires in large diameter and belowground biomass fuels, *J. Geophys. Res.*, *108*(D13), 8472, doi:10.1029/2002JD002100.

Boschetti, L., H. D. Eva, P. A. Brivio, and J. M. Grégoire (2004), Lessons to be learned from the comparison of three satellite-derived biomass burning products, *Geophys. Res. Lett.*, *31*, L21501, doi:10.1029/2004GL021229.

Brown, S., and G. Gaston (1995), Use of forest inventories and geographic information systems to estimate biomass density of tropical forests: Application to tropical Africa, *Environ. Monit. Assess.*, *38*, 157–168.

Cahoon, J., B. Stocks, J. Levine, W. Cofer, and K. O'Neill (1992), Seasonal distribution of African savannah fires, *Nature*, *359*, 812–815.

Desanker, P. V., P. G. H. Frost, C. O. Justice, and R. J. Schloes (Eds.) (1997), The Miombo Network: Framework for a terrestrial transect study of land-use and land-cover change in the Miombo ecosystems of Central Africa, Conclusions of the Miombo Network Workshop Zomba, Malawi, December 1995, *IGBP Rep. 41*, 109 pp., Int. Geosphere-Biosphere Programme, Stockholm, Sweden.

Di Gregorio, A., and L. Jansen (2000), Land cover classification system, classification concepts and user manual, Food and Agric. Org. of the U. N., Rome.

Gill, R. A., et al. (2002), Using simple environmental variables to estimate below-ground productivity in grasslands, *Global Ecol. Biogeogr.*, *11*, 79–86.

Goode, J. G., R. J. Yokelson, D. E. Ward, R. A. Susott, R. E. Babbitt, M. A. Davies, and W. M. Hao (2000), Measurements of excess O_3, CO_2, CO, CH_4, C_2H_4, C_2H_2, HCN, NO, NH_3, HCOOH, CH_3COOH, HCHO, and CH_3OH in 1997 Alaskan biomass burning plumes by airborne Fourier transform infrared spectroscopy (AFTIR), *J. Geophys. Res.*, *105*, 22,147–22,166.

Hansen, M. C., R. S. DeFries, J. R. G. Townshend, and R. Sohlberg (2000), Global land cover classification at 1 km spatial resolution using a classification tree approach, *Int. J. Remote Sens.*, *21*, 364–1331.

Hansen, M. C., R. S. DeFries, J. R. G. Townshend, R. Sohlberg, C. Dimiceli, and M. Carroll (2002a), Towards an operational MODIS continuous field of percent tree cover algorithm: Examples using AVHRR and MODIS data, *Remote Sens. Environ.*, *83*, 303–319.

Hansen, M. C., R. S. DeFries, J. R. G. Townshend, L. Marufu, and R. Sohlberg (2002b), Development of a MODIS tree cover validation data set for Western Province, Zambia, *Remote Sens. Environ.*, *83*, 320–335.

Hansen, M. C., R. S. DeFries, J. R. G. Townshend, M. Carroll, C. Dimiceli, and R. A. Sohlberg (2003), Global percent tree cover at a spatial resolution of 500 meters: First results of the MODIS vegetation continuous fields algorithm, *Earth Interactions*, *7*(10), 1–15.

Hao, W. M., M.-H. Liu, and P. J. Crutzen (1990), Estimates of annual and regional releases of CO_2 and other trace gases to the atmosphere from fires in the tropics, based on the FAO statistics for the period 1975–1980, in *Fire in the Tropical Biota: Ecosystem Processes and Global Challenges*, edited by J. G. Goldammer, pp. 440–462, Springer, New York.

Harmon, M. E., and C. Hua (1991), Coarse woody debris dynamics in two old-growth ecosystems, *BioScience*, *41*, 604–610.

Hély, C., S. Alleaume, R. J. Swap, H. H. Shugart, H. H. Shugart, and C. O. Justice (2003a), SAFARI-2000 characterization of fuels, fire behavior, combustion completeness, and emissions from experimental burns in infertile grass savannas in western Zambia, *J. Arid Environ.*, *54*, 381–394.

Hély, C., K. Caylor, S. Alleaume, R. J. Swap, and H. H. Shugart (2003b), Release of gaseous and particulate carbonaceous compounds from biomass burning during the SAFARI 2000 dry season field campaign, *J. Geophys. Res.*, *108*(D13), 8470, doi:10.1029/2002JD002482.

Hély, C., K. K. Caylor, P. R. Dowty, R. J. Swap, and H. H. Shugart (2003c), SAFARI 2000 modeled fuel load in Southern Africa 1999–2000, in *SAFARI 2000* [CD-ROM], *CD-ROM Ser.*, vol. 3, edited by J. Nickeson, D. Landis, and J. L. Privette, NASA Goddard Space Flight Cent., Greenbelt, Md. (Available from Oak Ridge Natl. Lab. Distributed Active Arch. Cent., Oak Ridge, Tenn.)

Hély, C., P. R. Dowty, S. Alleaume, K. K. Caylor, S. Korontzi, R. J. Swap, H. H. Shugart, and C. O. Justice (2003d), Regional fuel load for two climatically contrasting years in southern Africa, *J. Geophys. Res.*, *108*(D13), 8475, doi:10.1029/2002JD002341.

Hoelzemann, J. J., M. G. Schultz, G. P. Brasseur, C. Granier, and M. Simon (2004), The global wildland fire emission model GWEM: Evaluating the use of global area burnt data, *J. Geophys. Res.*, *109*, D14S04, doi:10.1029/2003JD003666.

Hoffa, E. A., D. E. Ward, W. M. Hao, R. A. Susott, and R. H. Wakimoto (1999), Seasonality of carbon emissions from biomass burning in a Zambian savanna, *J. Geophys. Res.*, *104*, 13,841–13,853.

Hurst, D. F., D. W. T. Griffith, and G. D. Cook (1994a), Trace gas emissions and biomass burning in tropical Australian savannas, *J. Geophys. Res.*, *99*, 16,441–16,456.

Hurst, D. F., D. W. T. Griffith, J. N. Carras, D. J. Williams, and P. J. Fraser (1994b), Measurements of trace gas emitted by Australian savanna fires during the 1990 dry season, *J. Atmos. Chem.*, *18*, 33–56.

Ito, A., and J. E. Penner (2004), Global estimates of biomass burning emissions based on satellite imagery for the year 2000, *J. Geophys. Res.*, *109*, D14S05, doi:10.1029/2003JD004423.

Jenkins, J. C., R. A. Birdsey, and Y. Pan (2001), Biomass and NPP estimation for the mid-Atlantic region (USA) using plot-level forest inventory data, *Ecol. Appl.*, *11*, 1174–1193.

Kanakidou, M., et al. (1999), 3-D global simulations of tropospheric CO distributions – Results of the GIM/IGAC intercomparison 1997 exercise, *Chemosphere Global Change Sci.*, *1*, 263–282.

Kasischke, E., and J. E. Penner (2004), Improving global estimates of atmospheric emissions and biomass burning, *J. Geophys. Res.*, *109*, D14S01, doi:10.1029/2004JD004972.

Korontzi, S., D. E. Ward, R. A. Susott, R. J. Yokelson, C. O. Justice, P. V. Hobbs, E. A. H. Smithwick, and W. M. Hao (2003), Seasonal variation and ecosystem dependence of emission factors for selected trace gases and PM2.5 for southern African savanna fires, *J. Geophys. Res.*, *108*(D24), 4758, doi:10.1029/2003JD003730.

Korontzi, S., D. P. Roy, C. O. Justice, and D. E. Ward (2004), Modeling and sensitivity analysis of fire emissions in southern Africa during SAFARI 2000, *Remote Sens. Environ.*, *92*, 376–396.

Lindesay, J. A., M. O. Andreae, J. G. Goldammer, G. Harris, H. J. Annegarn, M. Garstang, R. J. Scholes, and B. W. van Wilgen (1996), International Geosphere-Biosphere Programme/International Global Atmospheric Chemistry SAFARI-92 field experiment: Background and overview, *J. Geophys. Res.*, *101*(D19), 23,521–23,530.

Loveland, T. R., B. C. Reed, J. F. Brown, D. O. Ohlen, J. Zhu, L. Yang, and J. W. Merchant (2000), Development of a global land cover characteristics database and IGBP DISCover from 1 km AVHRR Data, *Int. J. Remote Sens.*, *21*, 1303–1330.

Matthews, E. (1983), Global vegetation and land use: New high-resolution data bases for climate studies, *J. Clim. Appl. Meteorol.*, *22*, 474–487.

Matthews, E. (1997), Global litter production, pools, and turnover times: Estimates from measurement data and regression models, *J. Geophys. Res.*, *102*, 18,771–18,800.

Mayaux, P. E. Bartholomé, S. Fritz, and A. Belward (2004), A new land-cover map of Africa for the year 2000, *J. Biogeogr.*, *31*, 861–877.

Menaut, J. C., L. Abbadie, F. Lavenu, P. Loudjani, and A. Podaire (1991), Biomass burning in west African savannas, in *Global Biomass Burning, Atmospheric, Climatic, and Biospheric Implications*, edited by J. S. Levine, pp. 133–142, MIT Press, Cambridge, Mass.

Myneni, R. B., R. R. Nemani, and S. W. Running (1997), Estimation of global leaf area index and absorbed par using radiative transfer models, *IEEE Trans. Geosci. Remote Sens.*, *35*, 1380–1393.

Palacios-Orueta, A., A. Parra, E. Chuvieco, and C. Carmona-Moreno (2004), Remote sensing and geographic information systems methods for global spatiotemporal modeling of biomass burning emissions: Assessment in the African continent, *J. Geophys. Res.*, *109*, D14S09, doi:10.1029/2004JD004734.

Penner, J. E., et al. (2002), A comparison of model- and satellite-derived aerosol optical depth and reflectivity, *J. Atmos. Sci.*, *59*, 441–460.

Pereira, J. M. C., A. C. L. Sa, J. M. N. Silva, D. E. Ward, and N. Riberio (2002), Biomass burning parameters of four experimental fires in the Western Province, Zambia, paper presented at SAFARI 2000 Synthesis Workshop, Univ. of Va., Charlottesville.

Pétron, G., C. Granier, B. Khattatov, V. Yudin, J. Lamarque, L. Emmons, J. Gille, and D. P. Edwards (2004), Monthly CO surface sources inventory based on the 2000–2001 MOPITT satellite data, *Geophys. Res. Lett.*, *31*, L21107, doi:10.1029/2004GL020560.

Roads, J. O., et al. (2003), GCIP water and energy budget synthesis (WEBS), *J. Geophys. Res.*, *108*(D16), 8609, doi:10.1029/2002JD002583.

Roy, D. P. (2003), SAFARI 2000 July and September MODIS 500 m burned area products for Southern Africa, in *SAFARI 2000* [CD-ROM], *CD-ROM Ser.*, vol. 3, edited by J. Nickeson, D. Landis, and J. L. Privette, NASA Goddard Space Flight Cent., Greenbelt, Md. (Available from Oak Ridge Natl. Lab. Distributed Active Arch. Cent., Oak Ridge, Tenn.)

Roy, D. P., P. E. Lewis, and C. O. Justice (2002), Burned area mapping using multi-temporal moderate spatial resolution data—A bi-directional reflectance model-based expectation approach, *Remote Sens. Environ.*, *83*, 263–286.

Saket, M. (2001), Wood volume and woody biomass, in *Global Forest Resources Assessment 2000*, edited by A. Perlis, pp. 17–22, For. and Agric. Org. of the U. N., Rome.

Scholes, R. J., J. Kendall, and C. O. Justice (1996a), The quantity of biomass burned in southern Africa, *J. Geophys. Res.*, *101*, 23,667–23,676.

Scholes, R. J., D. E. Ward, and C. O. Justice (1996b), Emissions of trace gases and aerosol particles due to vegetation burning in southern hemisphere Africa, *J. Geophys. Res.*, *101*, 23,677–23,682.

Seiler, W., and P. J. Crutzen (1980), Estimates of gross and net fluxes of carbon between the biosphere and the atmosphere from biomass burning, *Clim. Change*, *2*, 207–247.

Shea, R. W., B. W. Shea, J. B. Kauffman, D. E. Ward, C. I. Haskins, and M. C. Scholes (1996), Fuel biomass and combustion factors associated with fires in savanna ecosystems of South Africa and Zambia, *J. Geophys. Res.*, *101*, 23,551–23,568.

Shirai, T., et al. (2003), Emission estimates of selected volatile organic compounds from tropical savanna burning in northern Australia, *J. Geophys. Res.*, *108*(D3), 8406, doi:10.1029/2001JD000841.

Simon, M., S. Plummer, F. F. Fierens, J. J. Hoelzemann, and O. Arino (2004), Burnt area detection at global scale using ATSR-2; The GLOBSCAR products and their qualifications, *J. Geophys. Res.*, *109*, D14S02, doi:10.1029/2003JD003622.

Sinha, P., P. V. Hobbs, R. J. Yokelson, D. R. Blake, S. Gao, and T. W. Kirchstetter (2004), Emissions from miombo woodland and dambo grassland savanna fires, *J. Geophys. Res.*, *109*, D11305, doi:10.1029/2004JD004521.

Swap, R. J., H. J. Annegarn, J. T. Suttles, M. D. King, S. Platnick, J. L. Privette, and R. J. Scholes (2003), Africa burning: A thematic analysis of the Southern African Regional Science Initiative (SAFARI 2000), *J. Geophys. Res.*, *108*(D13), 8465, doi:10.1029/2003JD003747.

Tansey, K., et al. (2004), Vegetation burning in the year 2000: Global burned area estimates from SPOT VEGETATION data, *J. Geophys. Res.*, *109*, D14S03, doi:10.1029/2003JD003598.

van der Werf, G. R., J. T. Randerson, G. J. Collatz, and L. Giglio (2003), Carbon emissions from fires in tropical and subtropical ecosystems, *Global Change Biol.*, *9*, 547–562.

Ward, D. E., R. A. Susott, J. B. Kauffman, R. E. Babbitt, D. L. Cummings, B. Dias, B. N. Holden, Y. J. Kaufman, R. A. Rasmussen, and A. W. Setzer (1992), Smoke and fire characteristics for Cerrado and deforestation burns in Brazil: BASE-B experiment, *J. Geophys. Res.*, *97*(D13), 14,601–14,619.

Ward, D. E., W. M. Hao, R. A. Susott, R. E. Babbitt, R. W. Shea, J. B. Kauffman, and C. O. Justice (1996), Effect of fuel composition on combustion efficiency and emission factors for African savanna ecosystems, *J. Geophys. Res.*, *101*, 23,569–23,576.

Yokelson, R. J., I. T. Bertschi, T. J. Christian, P. V. Hobbs, D. E. Ward, and W. M. Hao (2003), Trace gas measurements in nascent, aged, and cloud-processed smoke from African savanna fires by airborne Fourier transform infrared spectroscopy (AFTIR), *J. Geophys. Res.*, *108*(D13), 8478, doi:10.1029/2002JD002322.

Zeng, X., R. E. Dickinson, A. Walker, M. Shaikh, R. S. DeFries, and J. Qi (2000), Derivation and evaluation of global 1-km fractional vegetation cover data for land modeling, *J. Appl. Meteorol.*, *39*, 826–839.

Zhu, Z., and E. Waller (2001), FRA 2000 global forest cover mapping final report, in *Forest Resource Assessment Programme*, edited by P. Pugliese, *Working Pap. 50*, For. and Agric. Org. of the U. N., Rome.

A. Ito, Frontier Research Center for Global Change, JAMSTEC, 236-0001 Yokohama, Japan. (akinorii@jamstec.go.jp)

J. E. Penner, Department of Atmospheric, Oceanic, and Space Sciences, University of Michigan, Ann Arbor, MI 48109-1349, USA.